Subtidal Variability of Estuarine Outflow, Plume, and Coastal Current: A Model Study

LIE-YAUW OEY

Department of Civil, Environmental, and Coastal Engineering, Stevens Institute of Technology, Hoboken, New Jersey

G. L. MELLOR

Atmospheric and Oceanic Sciences Program, Princeton University, Princeton, New Jersey

16 December 1991 and 3 April 1992

ABSTRACT

The time evolution of an estuary plume and its coastal front over a continental shelf is numerically calculated here using a three-dimensional model with eddy mixing based on the turbulence kinetic energy closure. The plume and front system is found to be unsteady with a natural period of about 5–10 days, during which the plume pulsates and intermittent coastal currents propagate down the coast.

1. Introduction

When light estuarine water debouches into an adjacent sea, a plume is formed at the mouth of the estuary. For wide estuaries, the earth's rotation becomes important and the discharged plume turns to the right (in the Northern Hemisphere) from the viewpoint of an observer at the estuary mouth looking seaward. A coastal front/current approximately 10 km wide is thus formed along the right-hand shoreline, carrying light water over great distances downcoast. This note presents results from a three-dimensional, time-dependent numerical simulation to illustrate some of the subtidal dynamics of the plume and its coastal current. We wish to study if the system is steady and what the temporal and spatial scales are.

2. The problem

We study here the dynamics of a large estuary plume and coastal front. By "large" we mean that the ratio K of the width of the estuary mouth to the baroclinic deformation radius R_0 is approximately one, or larger (Garvine 1987). Here $R_0 = C_i/f$, where C_i is the phase speed of the first baroclinic wave produced as a result of the density difference between fresh- and saltwater, and f is the Coriolis frequency arising from earth's rotation. A rough estimate for C_i is 1–2 m s^{-1} corresponding to a water depth of 20 m and a density difference of 5–20 kg m^{-3}, while $f \approx 10^{-4}$ s^{-1} for mid-latitude estuaries, so that $R_0 \approx$ 10–20 km. Thus, the Hudson, Delaware, and Chesapeake estuaries on the east coast of the United States and the Yangtse River into the East China Sea are large, since $K \geq 1$ in all cases. Physically, one may imagine that the discharged plume extends out into the ocean a distance of $O(R_0)$ before bending to the right and falling back toward the coast in a coastal front/current [also of width $O(R_0)$] that can meander as it travels down the coastline.

A three-dimensional numerical study of estuary plume has been conducted by Chao and Boicourt (1986) using the Bryan–Cox three-dimensional, primitive equation model with simple turbulence parameterization: constant vertical diffusivity/viscosity for stable stratification, and infinite mixing when unstable. The model consists of a closed-basin (north–south oriented) continental shelf connected at its western boundary through a 15-km opening to a channel estuary into which freshwater discharges at its westernmost end. After initial transients lasting about 5–10 days, an anticyclonic plume is formed over the shelf near the estuary mouth. The plume is quasi-steady in that no major time-dependent events occur thereafter, save the shedding of a few small-scale eddies at the fringe of the plume. The important contribution of Chao and Boicourt's work, however, is in their recognition that the plume dynamics is nonlinear and, therefore, that the transition from the plume to the coastal current downcoast occurs abruptly in a nearshore cyclonic surface flow region south of the estuary mouth. This description of the flow is different from that obtained in models with linear dynamics (Beardsley and Hart 1978; Ikeda 1984; Zhang et al. 1987) in which a smooth connection exists between the estuarine source and downcoast current.

Corresponding author address: Dr. Lie-Yauw Oey, Department of Civil, Environmental, and Coastal Engineering, Stevens Institute of Technology, Hoboken, NJ 07030.

Chao and Boicourt's model is unsteady, viscous, and weakly nonlinear. Garvine (1987), on the other hand, emphasizes steady, nonlinear, inviscid dynamics. The flow in the plume is anticyclonic and is bounded by a strong front. The cyclonic transition region south of the estuary mouth also exists in Garvine's model; moreover, stationary waves are found along the coastal current.

In this study, we extend the works of Chao and Boicourt (1986) and Garvine (1987) by presenting results from a model with unsteady, nonlinear, low-viscosity dynamics of the plume and coastal current system.

3. Methodology

The model domain, shown in Fig. 1, consists of a storage basin into which freshwater is pumped and that connects through an estuary, 39 km long and 15 km wide, to a continental shelf with a shoreline length of 700 km and width of 120 km. The alongshore distribution is interpreted as being oriented north to south. To simplify the model physics the ocean depth is set constant at 20 m.

The plume–coastal current problem is computationally difficult. First, one must simultaneously deal with small-scale turbulent processes, which laboratory experiments show to be important across the fresh–saline water boundary, as well as with large-scale plume and frontal physics. Here we parameterize the turbulent mixing process based on the turbulence kinetic energy and length-scale equations—the 2.5-level closure scheme of Mellor and Yamada (1982). To ensure that instability processes due to both the horizontal velocity shears and density gradients (or the vertical velocity shears) are properly taken into account, we use high-resolution grid of $\Delta z = 2$ m in the vertical and mini-

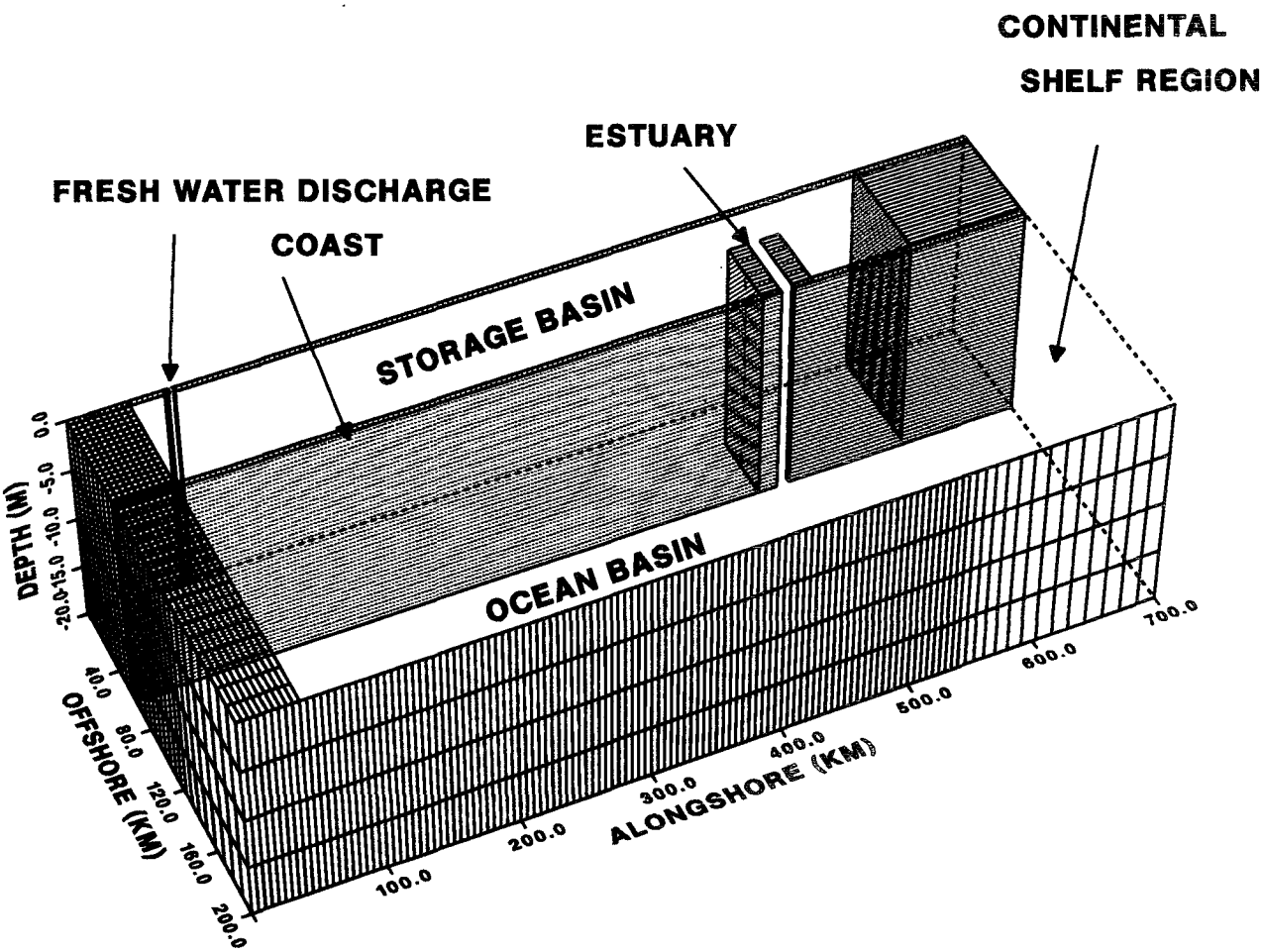

FIG. 1. The model domain. For clarity, only four levels in the vertical, and every other point in the finest horizontal grid are shown.

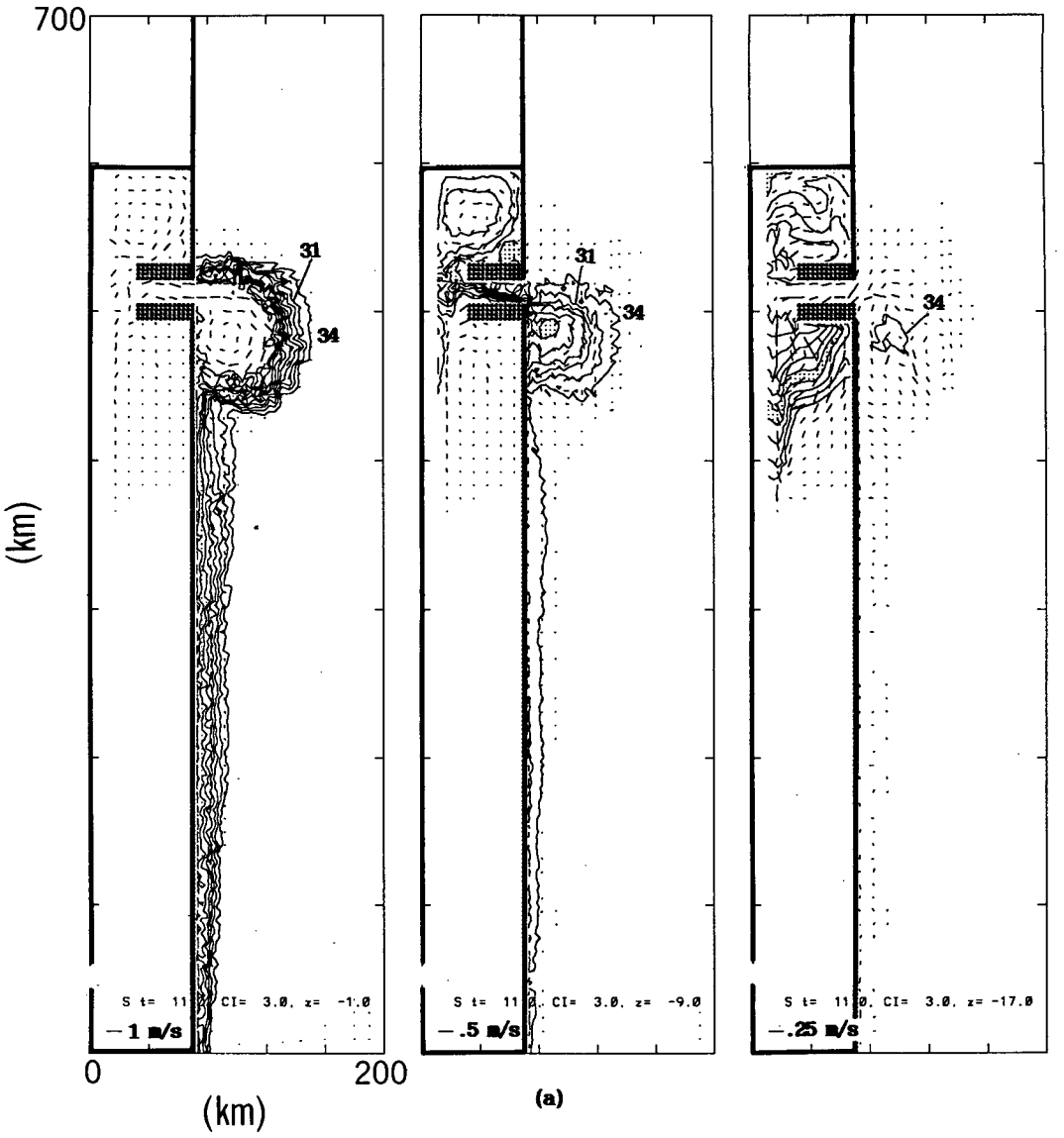

FIG. 2. Salinity contours/velocity vectors at $z = -1$ -9 and -17 m, for (a) $t = 11$ and (b) $t = 21$ days. Contour interval is 3 ppt: outermost contour on the shelf is 34 ppt. Vectors are plotted every other third point; heads or tails omitted for clarity. The length of the short line at the lower left-hand corner of each panel gives the vector scale.

mum horizontal grid sizes of $\Delta x = \Delta y = 3$ km (Fig. 1). Past experience with the model (Oey et al. 1985; Oey 1988) shows that this resolution is sufficient to resolve scales expected to be of $O(R_0)$.

Second, the problem is highly nonlinear, since supercritical flows often predominate (Garvine 1987). We therefore employ the (incompressible) Navier–Stokes equation on a rotating frame simplified only by the hydrostatic and Boussinesq assumptions, but retaining the important advective terms, both in the momentum and the salinity and temperature equations. (The system is sometimes referred to as the primitive equation.) The model equations and the method of solution are given in Blumberg and Mellor (1983) and Oey et al. (1985). The model also contains planetary beta; however, its effect is negligible in the spatial and temporal scales being examined.

Finally, open boundaries around the continental shelf must be such that energetic bores that propagate along the coast are allowed to pass through. This turned out to be nontrivial, especially for the southern cross-shelf boundary. We experimented with various schemes and finally used a radiation condition (Orlanski 1976) coupled with enhanced alongshore diffusion across the southern transect. This implementation of the open boundary conditions is important for at least two reasons. First, long-term integration of subtidal variability with periods of days to months becomes feasible, and second, mixing processes due to tides and winds can be included. The model has in fact now been applied

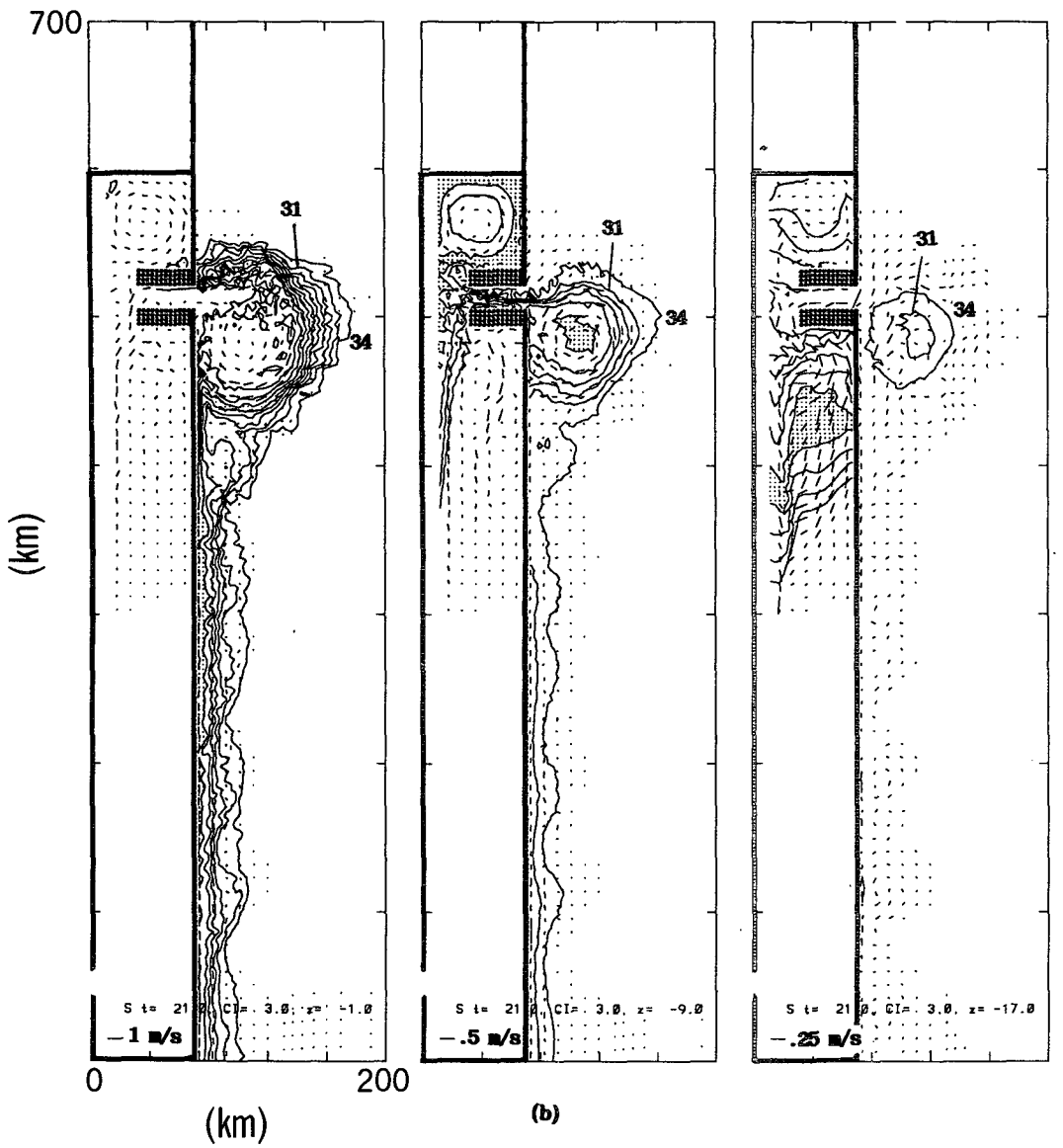

FIG. 2. (*Continued*)

to a one-year simulation of the circulation and mixing in the New York Bight (You et al. 1991; Chen et al. 1991).

At time $t = 0$, the ocean basin, including the connecting estuary, is filled with saltwater of 35 psu, and the storage basin with freshwater (salinity: 0 psu). The temperature of the two water masses is fixed at 10°C, and the corresponding density difference is about 28 kg m^{-3}. For $t > 0$, calculation continues for 80 days as freshwater from the estuary head spreads over, and mixes with, the saline ocean water.

4. Results

Figure 2 shows the computed salinity contours and velocity vectors at $z = -1$, -9, and -17 m and at (a) $t = 11$ and (b) 21 days. These show (i) a plume bounded by an intense semicircular front off the estuary mouth; in the plume, current rotates anticyclonically (clockwise), and inertia balances the Coriolis acceleration (Garvine 1987); (ii) a meandering coastal current that undergoes two stages of development in which (Fig. 2a) short wavelengths of $O(2R_0 \approx 20$ km) are seen and (Fig. 2b) longer wavelengths of $O(2\pi R_0)$ also appear. The short waves are similar to those found by Garvine (1987), although an exact comparison is not possible because of the unsteady nature of the present flow field. An energetic analysis indicates instability of barotropic (through horizontal shears; cf. Garvine 1987) and baroclinic (through vertical shears) origins, respectively, for the two stages, as can be expected from the two wavelength scales; and (iii) smooth exit of the coastal front/current across the southern boundary; a nonradiative condition would send the current anti-

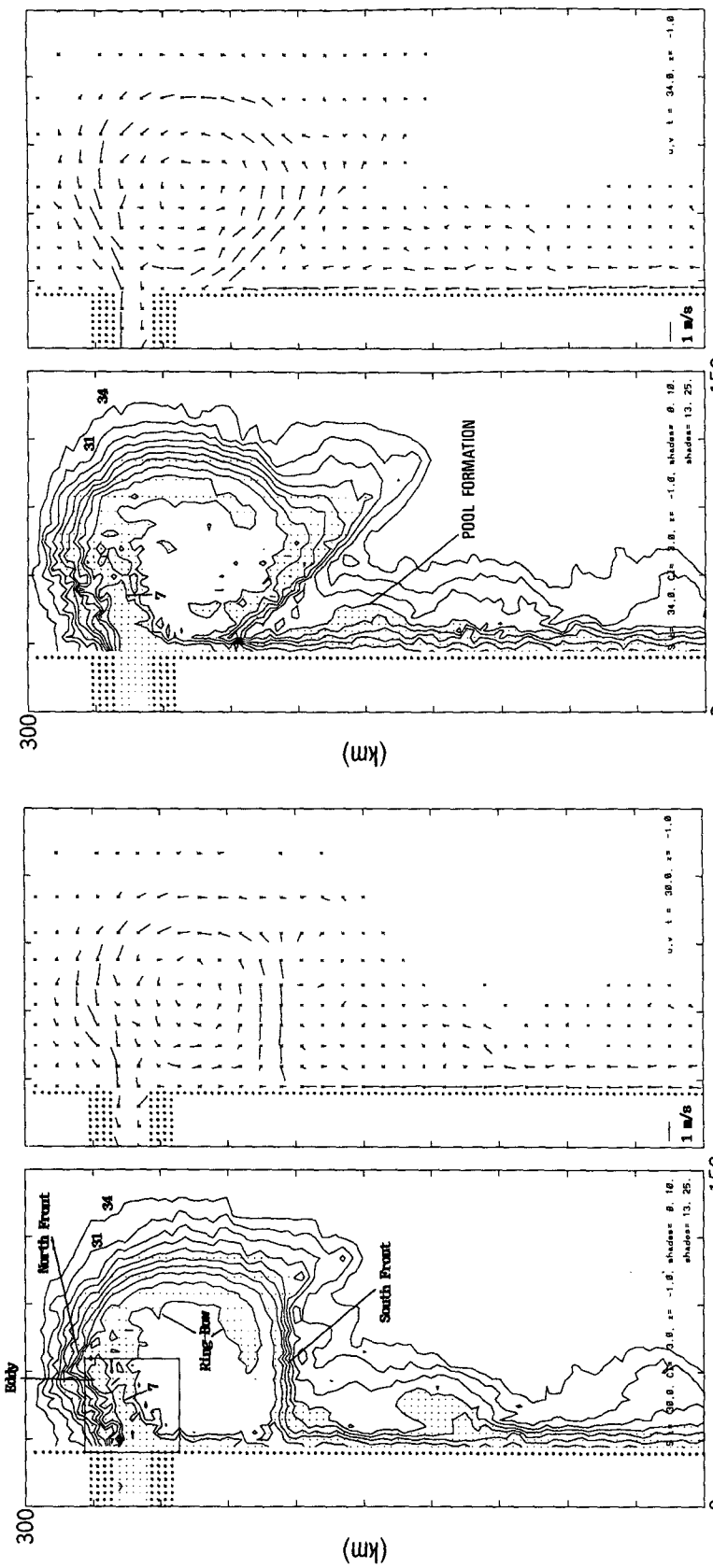

FIG. 3. Salinity contours and velocity vectors at $z = -1$ m, for time (a) 30 days, (b) 34 days, (c) 40 days, (d) 43 days, and (e) 47 days. The contour interval is 3 ppt: the outermost contour on the shelf is 34 ppt. Regions with salinity less than 10 ppt, and also between 13 ppt and 25 ppt are shaded. Velocity vectors are plotted at every other third point, and tails (denoting origin of flow directions) are marked by "x." The length of the short line at the lower left-hand corner of the velocity vector panel gives the scale of 1 m s^{-1}.

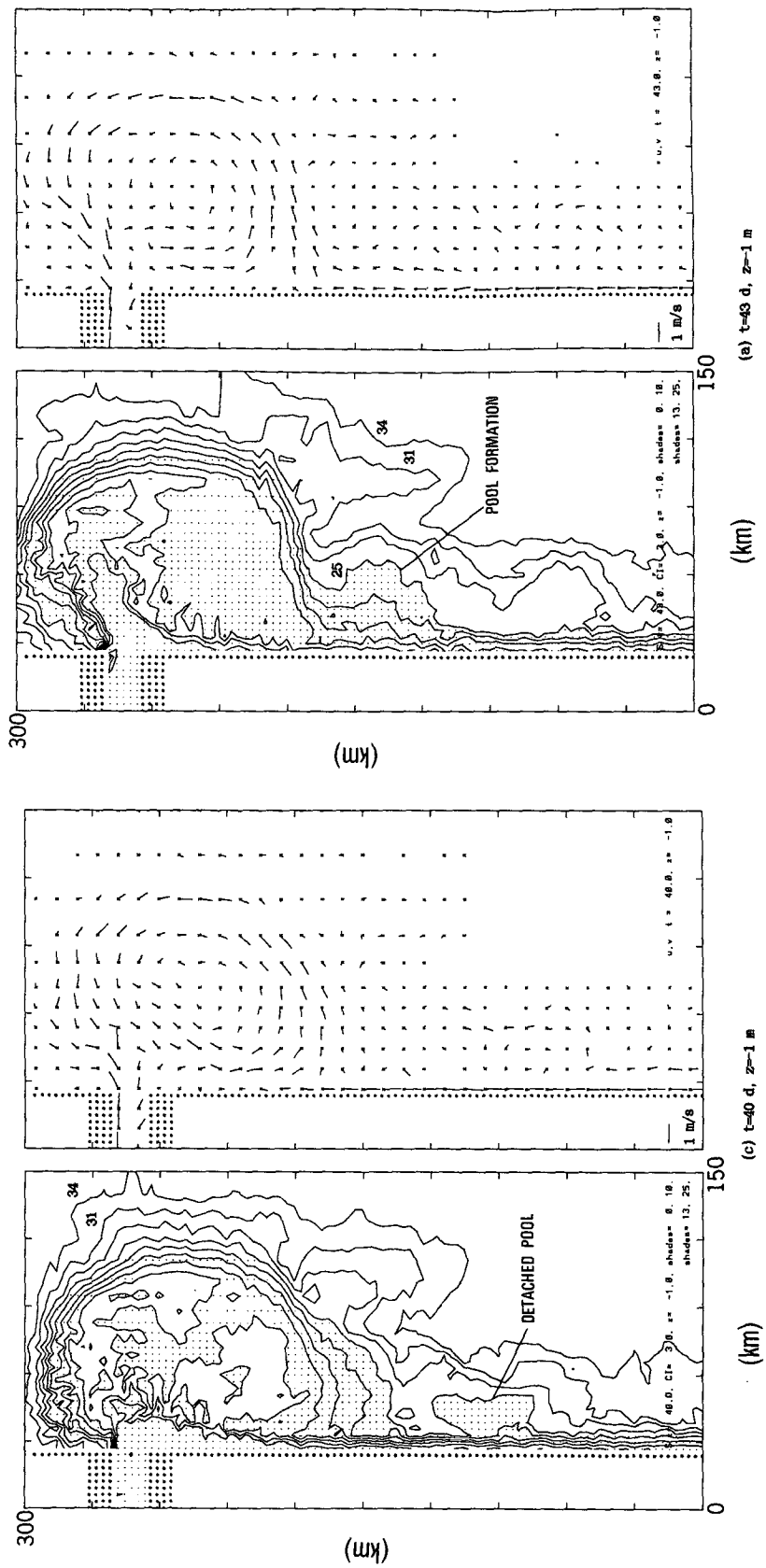

FIG. 3. (*Continued*)

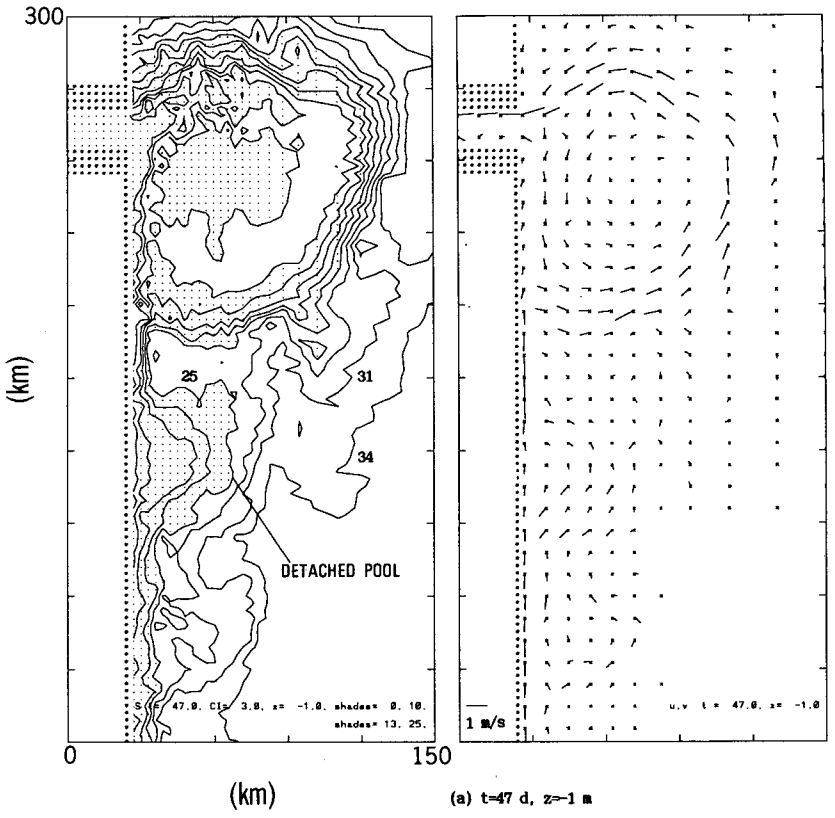

FIG. 3. (*Continued*)

clockwise 500 km along the open boundary from day 10 to day 20. The flow is highly nonlinear. First, outflow velocity at the estuary mouth reaches values ≥ 1 m s^{-1}, that is, near-critical to supercritical with respect to the first baroclinic wave mode, especially for flow exiting along the northern wall of the estuary (Fig. 2b). Second, the anticyclonic current abruptly turns cyclonically near the coast south of the estuary, which then acts as a transition zone connecting the plume and the coastal current farther south (Chao and Boicourt 1986). In models with linear dynamics, the coastal current connects smoothly to the plume after passage of the Kelvin wave (Beardsley and Hart 1978; Ikeda 1984). In the present case, on the other hand, an intrusive bore is formed propagating down the coast (Fig. 2).

We also performed a model run identical to the one described earlier except that the eddy viscosity/diffusivity are constant, as in Chao and Boicourt (1986). While there is a strong resemblance between the two calculations (the anticyclonic plume and cyclonic transition region), there are also important differences. Flows with the constant eddy mixing are always subcritical, and the resulting plume front is diffused. Also, the present calculation shows small-scale, surface pools of less-saline "rings" inside the plume—a result of internal hydraulic jumps and associated vertical mixing. A blow-up sequence of the salinity contours and velocity vector plots at $z = -1$ m in Fig. 3 shows this (see, in particular, Fig. 3a). The sequence also suggests a subtidal variability of the plume and coastal front, which we illustrate schematically in Fig. 4. At time t_1 the plume is strengthened by the discharge from the estuary. At time t_2 accumulation of buoyant water at SF eventually produces northward intrusion, and a strong cyclone is produced at the eye of intrusion just south of SF. Also, at this time, outflow from the estuary diminishes as pressure difference between the shelf and

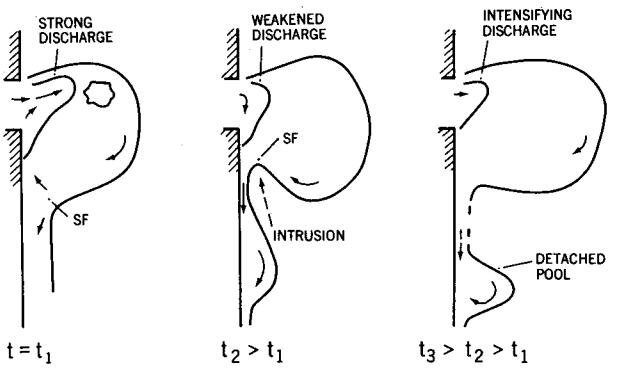

FIG. 4. A schematic of the different phases of development of the plume and its near-surface circulation: the strengthening phase $t = t_1$, the intrusion phase $t = t_2$, and the pool-detachment phase $t = t_3$.

TABLE 1. List of sensitivity experiments.

Experiment	Description	Results
1	Discussed in text	
2	Same as experiment 1 without the storage basin; freshwater discharge at head of estuary, plus radiation; calculation for 160 days.	Surface outflow becomes slightly stronger; plumes' variabilities (periods and spatial structures) remain basically unchanged.
3	Same as experiment 1 except that the southern cross-shelf boundary is located at 300 km instead of 500 km south of the estuary mouth; calculation for 60 days.	Solution is changed only near the (new) southern boundary where smooth exit is imposed by the diffusive radiation condition.
4	Same as experiment 1 except that the horizontal viscosity and diffusivity are changed from 10 $m^2 s^{-1}$ to (a) 1 $m^2 s^{-1}$, (b) 20 $m^2 s^{-1}$, (c) 80 $m^2 s^{-1}$, and (d) 160 $m^2 s^{-1}$; (a) and (b) were run for 60 days each, (c) for 100 days, and (d) for for 50 days. Laplacian-type diffusion is used in all the experiments.	For (a) and (b) the results are not much changed from experiment 1; for (c) the surface outflow is much weakened and there are almost no variabilities; for (d), flow becomes steady and the coastal current becomes wider.
5	Same as experiment 1 except that the last 10 alongshore grids near the southern cross-shelf boundary are variable, increasing linearly southward from 3 km to 10 km.	Spurious perturbations occur across the region of changing grid when the southward-propagating alongshore bore arrives.

estuary equilibrates, and discharge weakens. The cyclone at SF produces an intense southward jet inshore so that (i) velocity associated with the jet is much larger than that farther south and flow convergence occurs and (ii) buoyancy supply to the south peaks with the jet. The net result is that a meander grows south of the cyclone and in time, detaches as a shorebound pool of less-saline water that moves southward, as shown in Fig. 4 for time t_3. This process repeats with a period of about 10 days, and intermittent coastal current is produced as pools of less-saline water propagate downcoast.

In Figs. 3a–c, t_1 = 30 days is when the plume strengthens, t_2 = 34 days is at time of intrusion and pool formation, and t_3 = 40 days is when the pool has detached from the main plume. Figures 3d,e continue to the next cycle in which $t_1 < 43$ days $< t_2$ (Fig. 3d) and t_3 = 47 days (Fig. 3e). The formation of pool is clear from Fig. 3e. Thus, one obtains a succession of meanders along the coastal front. The amplitude of meander is about 15–30 km, and its wavelength is about 60–70 km. It is likely that these intermittent perturbations act to trigger the barotropic and baroclinic instabilities along the coastal front, previously mentioned in conjunction with Fig. 2.

In Table 1, we list various sensitivity experiments conducted to ascertain that the plume variability is not a function of the model geometry and setup. Note that because of problems encountered when using a variable grid near the southern boundary (experiment 5; the so-called "telescoping" grid) we used a constant grid in other experiments for the shelf region south of the estuary mouth.

5. Conclusions

Our results suggest that in addition to wind-induced motions, natural subtidal variability of plumes and coastal currents related to the system's dynamic instability may also be important in shelf circulation.

Acknowledgments. This research was sponsored by the Office of Science and Research of the NJDEP Contracts P25442 and P31006. LYO benefitted from discussions with J. Blanton of Skidaway Institute of Oceanography. Supercomputer time was provided by the National Center for Supercomputing Applications, Illinois, and the Pittsburgh Supercomputer Center.

REFERENCES

Beardsley, R. C., and J. Hart, 1978: A simple theoretical model for the flow of an estuary onto a continental shelf. *J. Geophys. Res.*, **83**, 873–883.

Blumberg, A. F. and G. L. Mellor, 1983: Diagnostic and prognostic numerical circulation studies of the South Atlantic Bight. *J. Geophys. Res.*, **88**, 4579–4592.

Chao, S.-Y., and W. C. Boicourt, 1986: Onset of estuarine plumes. *J. Phys. Oceanogr.*, **16**, 2137–2149.

Chen, P., Y.-H. Zhang, and L.-Y. Oey. A coastal-ocean forecast/hindcast model. *ASCE J. Hydraul.*,

Garvine, R. W., 1987: Estuary plumes and fronts in shelf waters: a layer model. *J. Phys. Oceanogr.*, **17**, 1877–1896.

Ikeda, M., 1984: Coastal flows driven by a local density flux. *J. Geophys. Res.*, **89**, 8008–8016.

Mellor, G., and T. Yamada, 1982: Development of a turbulence closure model for geophysical fluid problems. *Rev. Geophys. Space Phys.*, **20**, 851–875.

Oey, L.-Y., 1988: A model of Gulf Stream frontal instabilities, meanders and eddies along the continental slope. *J. Phys. Oceanogr.*, **18**, 211–229.

——, G. L. Mellor, and R. I. Hires, 1985: A three dimensional simulation of the Hudson-Raritan estuary. Part I: Description of the model and model simulations. *J. Phys. Oceanogr.*, **15**, 1676–1692.

Orlanski, I., 1976: A simple boundary condition for unbounded hyperbolic flows. *J. Comput. Phys.*, **21**, 251–269.

You, K.-W., Y.-H. Zhang, L.-Y. Oey, and others. 1992: A model simulation of the wind and buoyancy-driven circulation in the New York Bight/Harbor. *ASCE J. Hydraul.*,

Zhang, Q. H., G. S. Janowitz, and L. J. Pietrafesa, 1978: The interaction of estuarine and shelf waters: A model and applications. *J. Phys. Oceanogr.*, **17**, 455–469.